doi:10.1093/jmcb/mjv046
Published online June 27, 2015

Article

E-selectin ligand complexes adopt an extended high-affinity conformation

Roland C. Preston[1], Roman P. Jakob[2], Florian P.C. Binder[1], Christoph P. Sager[1], Beat Ernst[1,*], and Timm Maier[2,*]

[1] Institute of Molecular Pharmacy, Universität Basel, 4056 Basel, Switzerland
[2] Biozentrum, Universität Basel, 4056 Basel, Switzerland
* Correspondence to: Timm Maier, E-mail: timm.maier@unibas.ch; Beat Ernst, E-mail: beat.ernst@unibas.ch

E-selectin is a cell-adhesion molecule of the vascular endothelium that promotes essential leukocyte rolling in the early inflammatory response by binding to glycoproteins containing the tetrasaccharide sialyl Lewis^x (sLe^x). Efficient leukocyte recruitment under vascular flow conditions depends on an increased lifetime of E-selectin/ligand complexes under tensile force in a so-called catch-bond binding mode. Co-crystal structures of a representative fragment of the extracellular E-selectin region with sLe^x and a glycomimetic antagonist thereof reveal an extended E-selectin conformation, which is identified as a high-affinity binding state of E-selectin by molecular dynamics simulations. Small-angle X-ray scattering experiments demonstrate a direct link between ligand binding and E-selectin conformational transition under static conditions in solution. This permits tracing a series of concerted structural changes connecting ligand binding to conformational stretching as the structural basis of E-selectin catch-bond-mediated leukocyte recruitment. The detailed molecular view of the binding site paves the way for the design of a new generation of selectin antagonists. This is of special interest, since their therapeutic potential was recently demonstrated with the pan-selectin antagonists GMI-1070 (Rivipansel).

Keywords: inflammation, leukocyte adhesion, E-selectin, glycomimetic antagonist, sialyl Lewis^x, conformational change

Introduction

E-, P-, and L-selectin are a family of Ca^{2+}-dependent C-type lectins mediating cell-cell adhesion in the vascular system with a pivotal role in inflammation (Lasky, 1995). They are expressed on the vascular endothelium (E-, P-selectin), platelets (P-selectin), or leukocytes (L-selectin) and bind to cell-surface glycoproteins, e.g. P-selectin glycoprotein ligand-1 (PSGL-1) or E-selectin ligand-1 (ESL-1) presenting the minimal tetrasaccharide binding motif sialyl Lewis^x (sLe^x, Figure 1A) (Phillips et al., 1990; Walz et al., 1990; Polley et al., 1991). Selectins exhibit catch-bond behavior: The lifetime of complexes of selectins with their ligands increases under tensile force conditions (Thomas et al., 2008) as demonstrated first by atomic force microscopy and flow chamber assays for P-selectin (Marshall et al., 2003; Waldron and Springer, 2009), later also for L-selectin (Finger et al., 1996; Ramachandran et al., 1999; Sarangapani et al., 2004; Lou et al., 2006; Zhu et al., 2008), and most recently for E-selectin (Snook and Guilford, 2010; Wayman et al., 2010). For E- and P-selectin, the catch-bond binding mode is required under flow conditions for efficient leukocyte tethering and rolling along the vascular endothelium, a prerequisite for subsequent firm adhesion and transmigration to sites of inflammation (Kansas, 1996). Due to their essential role in leukocyte recruitment, selectins are an attractive target for therapeutic intervention against diseases involving excessive inflammatory response as found in numerous cardiovascular and autoimmune diseases (Ley, 2003). A first demonstration of the therapeutic potential of selectin inhibition was very recently achieved by successful completion of phase-II clinical trials of the pan-selectin antagonists GMI-1070 (Rivipansel) for the treatment of the vaso-occlusive crisis in sickle-cell disease (Clinicaltrials.gov, 2014a, b). The success of GMI-1070 now paves the way for the development of selectin type-specific antagonists for further indications.

The selectins share a conserved domain architecture (Figure 1B) with an N-terminal lectin (Lec) domain, which contains the carbohydrate-binding site, an epidermal growth factor (EGF)-like domain, variable numbers of short consensus repeat (SCR) domains, a single-span transmembrane region, and a C-terminal cytoplasmic domain. Isolated Lec-EGF didomain fragments are sufficient for ligand binding (Erbe et al., 1992); however, as demonstrated in cell-based assays, their affinity improves with an increasing number of

Received December 23, 2014. Revised April 1, 2015. Accepted April 27, 2015.

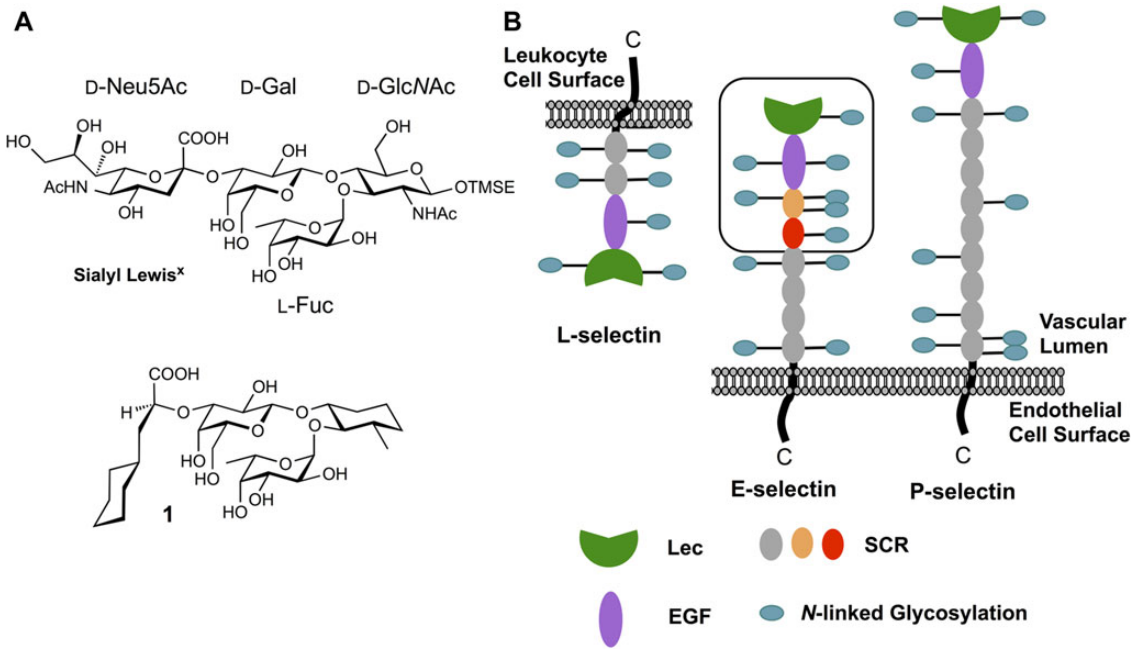

Figure 1 E-selectin ligands and selectin domain arrangement. (**A**) Chemical structures of sialyl Lewis^x (sLe^x) and glycomimetic **1** (Schwizer et al., 2012). (**B**) Comparison of human L-, E-, and P-selectin. The representative E-selectin fragment used in this publication (E-selectin*) is boxed and domains are colored red, orange (SCR domains), magenta (EGF), and green (lectin) as in following figures.

attached SCR domains (Li et al., 1994). Several models have been established to link the catch-bond phenomenon to the structure of selectins and their ligands. In the sliding-rebinding model, the alignment of the binding interface to the tensile force allows the ligand to slide along the protein surface and continuously form new interactions (Lou et al., 2006; Lou and Zhu, 2007). Other models build upon an allosteric relationship between force-induced domain separation and conformational changes in the binding site (Thomas et al., 2006; Yakovenko et al., 2008; Springer, 2009). In the one-state-two-pathway model, a single low-energy state exists under no-force conditions with a high rate of unbinding (Pereverzev et al., 2005). When force is applied, the protein switches into a conformation with a decreased rate of unbinding, thus allowing for longer lifetimes of the interactions. In the two-state-two-pathway model, high- and low-affinity conformations are in equilibrium under no-force conditions and the ligand can dissociate from either conformational state, albeit at different rates (Evans et al., 2004; Beste and Hammer, 2008). Under force conditions, the high-affinity state is preferred, leading to decreased unbinding up to a certain force threshold.

Currently, a single conformational state of the Lec-EGF didomain has been visualized for apo-P- and E-selectin as well as for sLe^x-bound P- and E-selectin in crystallographic soaking experiments (Graves et al., 1994; Somers et al., 2000). However, the crystal structure of the P-selectin Lec-EGF didomain co-crystallized with a large tyrosine-sulfated glycopeptide fragment of its physiological glycoprotein ligand PSGL-1, yielded a second, more extended conformation, suggesting a mechanism of conformational coupling specific for the binding of P-selectin to its multivalent peptide ligand (Somers et al., 2000). It remains unclear how catch-bond behavior is mediated in E- and L-selectin and whether small-molecule ligands are capable of mediating conformational transitions. To analyze the crosstalk between conformational changes and binding of the natural tetrasaccharide epitope sLe^x and the glycomimetic **1** (Figure 1A) to E-selectin, we used a representative four-domain fragment (E-selectin*) of the extracellular region of E-selectin comprising the Lec and EGF-like domains as well as two SCR domains. While sLe^x has a weak affinity for E-selectin (K_D 878 μM), glycomimetic **1** exhibits an enhanced affinity in the low micromolar range (K_D 19 μM) (Binder et al., 2012). Here, sialic acid and *N*-acetyl-D-glucosamine (Glc*N*Ac) are replaced by (*S*)-cyclohexyl lactic acid and (1*R*,2*R*,3*S*)-3-methylcyclohexane-1,2-diol, respectively. Combining structural information from co-crystallizing E-selectin* with sLe^x or glycomimetic **1** with molecular dynamics simulations and solution small-angle X-ray scattering (SAXS), we reveal a novel high-affinity binding state relevant for catch-bond interactions in E-selectin and provide the basis for future rational drug design of potent E-selectin antagonists.

Results

To analyze the implications of ligand binding to E-selectin, we determined the crystal structures of a representative fragment of the E-selectin extracellular region (E-selectin*) with either sLe^x or the glycomimetic **1**. Secreted E-selectin* was expressed in CHO cells and purified by affinity chromatography with antibody *7A9*, which blocks E-selectin functionality (Rodriguez-Romero et al., 1998). The purified protein after deglycosylation (Supplementary Figure S1) contains single Glc*N*Ac residues attached to each of the seven predicted *N*-glycosylation sites and is functional in ligand binding assays (Supplementary Figures S2 and S3). E-selectin* co-crystals with

sLe^x or glycomimetic **1** were obtained in crystallization conditions based on polyethylene glycol 8000 in the presence of 0.2 M $CaCl_2$ and diffracted to 2.40 Å and 1.93 Å, respectively. Structure determination was carried out by molecular replacement, final structures were refined to R_{work}/R_{free} 0.217/0.253 and 0.183/0.232 for sLe^x and glycomimetic **1** co-crystals, respectively, with two virtually identical molecules per asymmetric unit (Supplementary Table S1). Omit electron density maps for the ligand-binding site and hinge regions are shown in Supplementary Figure S4.

E-selectin ligand complexes adopt an extended linear conformation

Both ligand complexes of E-selectin* adopt an extended shape with a total length of 135 Å (Figure 2A). The binding modes of the physiological sLe^x ligand and glycomimetic **1** are almost identical (Figure 3A); both ligands bind into the same deep binding pocket covered by the loop 83–88, and their L-fucose moieties coordinate the central Ca^{2+} ion of the Lec domain. However, compared with previously published structures of E-selectin Lec-EGF didomain fragments (Graves et al., 1994; Somers et al., 2000), either without ligand or with sLe^x soaked into preformed protein crystals, considerable rearrangements in the ligand-binding site and a transition from a bent to an extended shape of the Lec-EGF didomain are observed (Figure 3B). The SCR domains, which have not been previously visualized in the context of selectin Lec-EGF didomains, align in both ligand complexes in a linear fashion with the EGF domain (Figure 2B). Since E-selectin*/**1** crystals diffract to higher resolution, the discussion focuses on this complex.

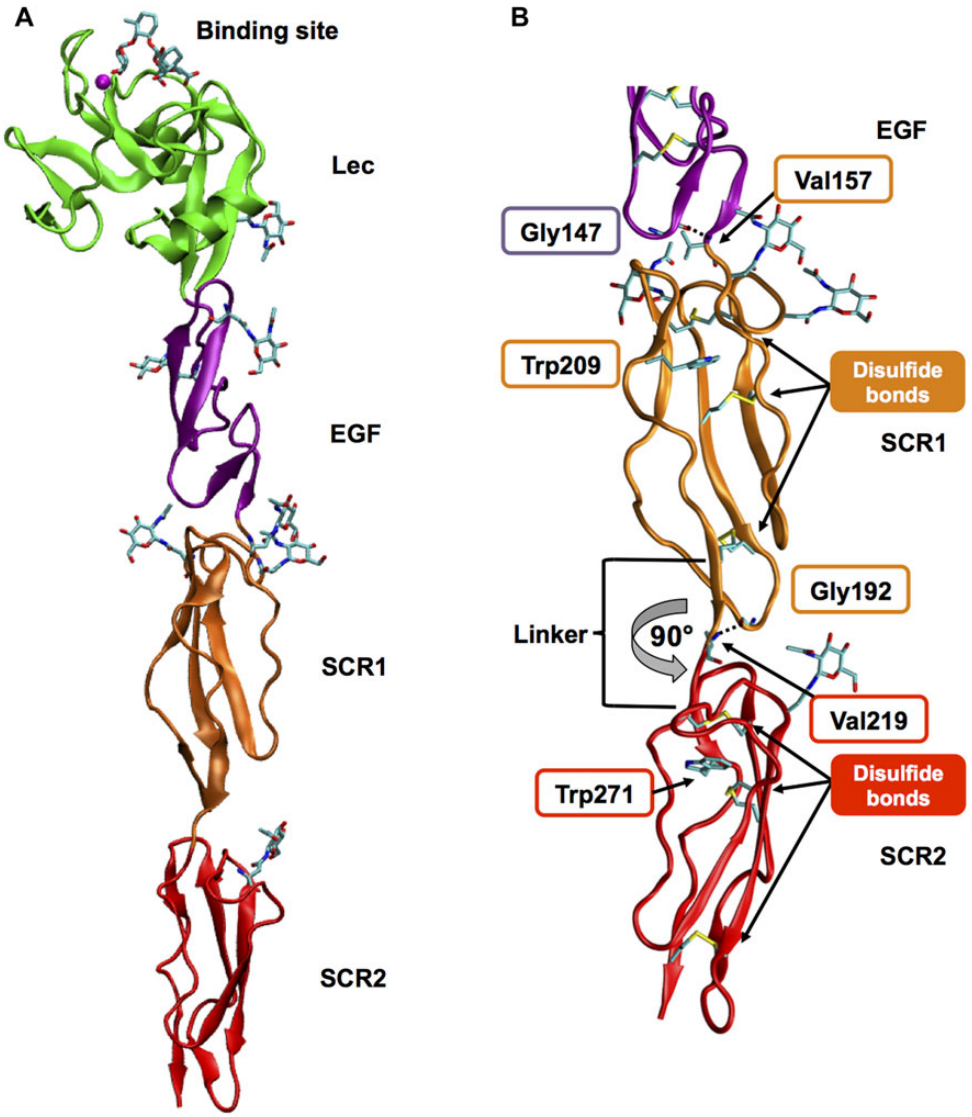

Figure 2 E-selectin short consensus repeat domains are linear rigidified domains. (**A**) Structure of E-selectin with the N-terminal Lec, the EGF-like, and the first two SCR domains. The glycomimetic **1** coordinates the Ca^{2+} ion (magenta) in the carbohydrate recognition site. Seven *N*-linked Glc*N*Ac moieties are located at interdomain interfaces. (**B**) The SCR domains are aligned, with a 90° rotation of SCR2 relative to SCR1. Three disulfide bonds stabilize each SCR domain. Conserved tryptophans (Trp209/271) are wedged between the upper and central disulfide bond. SCR domain flexibility is limited by hydrogen bonds between Gly147 and Val157 or Gly192 and Val219.

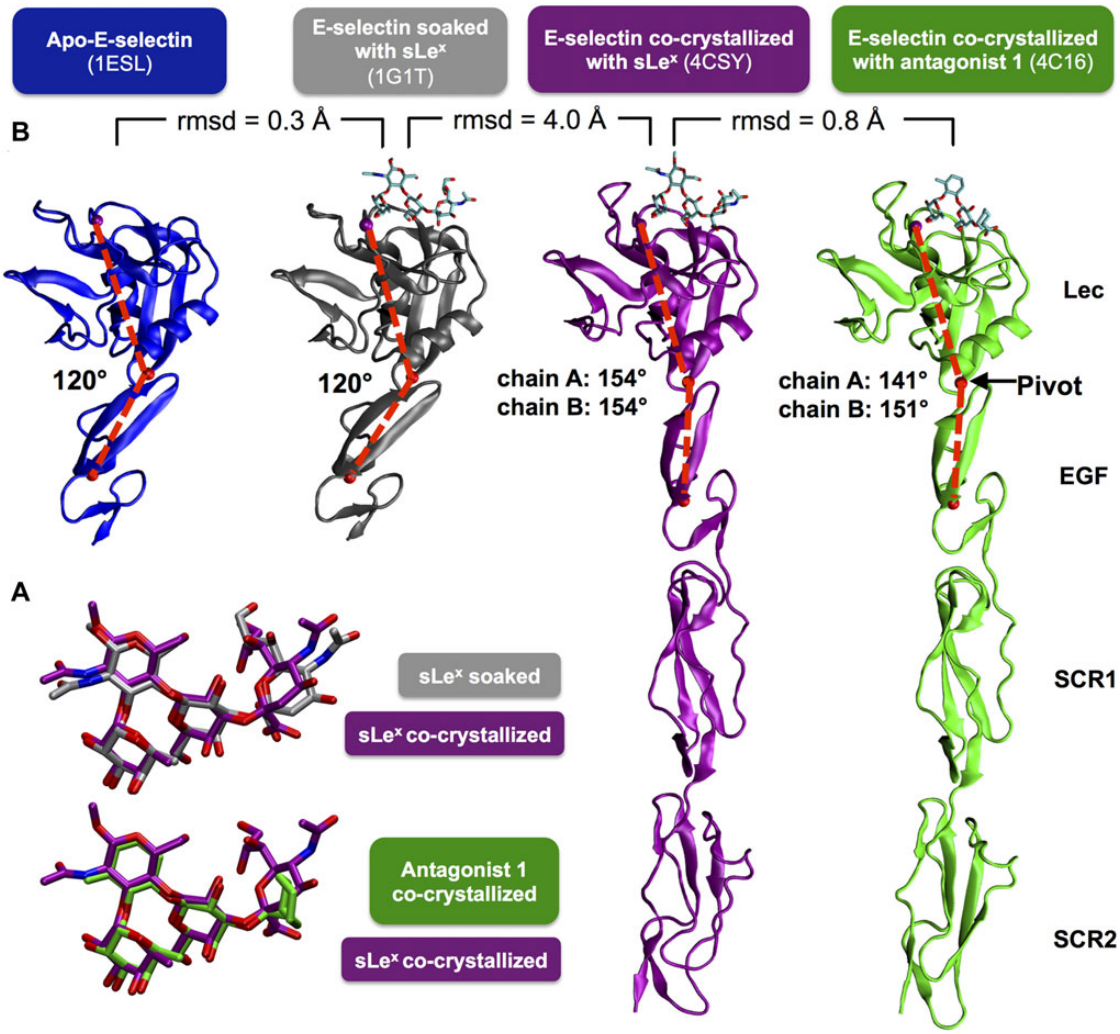

Figure 3 E-selectin adopts an extended overall conformation upon ligand binding. (**A**) Superposition of sLe^x soaked into preformed crystals (Somers et al., 2000) (gray, upper panel) and the co-crystallized glycomimetic **1** (green, lower panel) onto the co-crystallized sLe^x (purple). (**B**) Apo-E-selectin (blue, PDB code 1ESL) (Graves et al., 1994) and E-selectin soaked with sLe^x (gray, PDB code 1G1T) (Somers et al., 2000) adopt a bent conformation. The extended state observed in co-crystals with sLe^x (magenta) or glycomimetic **1** (green) is characterized by a separation of the Lec and EGF-like domains. Root-mean-square deviations (rmsd) were calculated for Lec and EGF-like domains only. The ligand-binding Ca^{2+} ion is depicted as a magenta sphere, Cα atoms of Trp1 (pivot) and Cys144 (EGF-like domain) as red spheres.

Rigidified short consensus repeats at the basis of the selectin extracellular domain

In selectins, between two and nine SCR domains provide the coupling of the Lec-EGF didomain to the cell surface. E-selectin comprises six SCR domains, two of which are included in E-selectin*. The sequence conservation of selectin SCR domains is low (Supplementary Figure S5); however, they all consist of a 60 amino acid compact β-sheet fold (Figure 2B) and contain six conserved cysteines, two more than most other SCR domains (Supplementary Table S5 and references therein). These cysteines form three intradomain disulfide bonds, two common ones at each end of the domain, and an additional disulfide bond in the center. A conserved tryptophan (SCR1:Trp209, SCR2:Trp271) is interlocked between the N-terminal and the central disulfide bond (Figure 2B) resulting in the formation of a tightly packed rigid core in selectin SCR domains. The two successive SCR domains are rotated by 90° relative to each other. This orientation is stabilized by an interaction of the loop Gly192 backbone oxygen with the backbone NH of the linker region Val219. A similar stabilizing interaction is observed at the EGF/SCR1 interface between Gly147 and Val157. The linker between the linearly arranged E-selectin SCR1-2 domains is composed of only four residues (Asn217, Val218, Val219, and Glu220), while linker lengths of five to eight residues have been observed in non-linearly arranged SCR domains (Prota et al., 2002). In contrast to SCR domain linkers in other proteins, the pattern of hydrophilic-hydrophobic-hydrophobic-hydrophilic amino acids is well conserved in all selectin SCR linkers, except between SCR7 and 8 in P-selectin (Supplementary Figure S5), indicating a critical role of linker composition and stabilizing interdomain interactions for selectin function.

The first E-selectin SCR domain possesses three *N*-linked glycosylation sites (Asn158, Asn178, Asn182), while the second SCR2 has a single site (Asn244). The observed glycosylation sites are located at the interface of the EGF-like/SCR1 and SCR1/SCR2 domains. While SCR4 and SCR5 have no predicted glycosylation sites, SCR3 and SCR6 each carry two at position 291, 311 (SCR3) and 482, 506 (SCR6). Based on the SCR1/2 structure, glycosylation at residue 291 is located at the interface to SCR2, and both sites in SCR6 are in close proximity to the membrane surface. This arrangement indicates that glycosylation may contribute to protection of exposed SCR domain linking regions against proteolytic cleavage, as generally observed for other glycosylated proteins (Imperiali and O'Connor, 1999; Kundra and Kornfeld, 1999; Crothers et al., 2004). Together with the conserved tryptophans, the additional disulfide bond and the conserved linker region, glycosylation thus contributes to the formation of a reinforced SCR stalk for mechanosensing by the Lec-EGF didomain.

Ligand binding induces the extended high-affinity conformation of E-selectin

The relative orientation of the Lec and EGF domains observed here in both ligand complexes is considerably different from the bent conformation observed previously in crystals of a E-selectin Lec-EGF didomain fragment without ligand or soaked with sLe^x (Graves et al., 1994; Somers et al., 2000). In the bent conformation, the angle between the Lec and EGF domains is ~120°, while it is 141° and 151° in the current co-crystal structures (Figure 3B and Supplementary Video S1). This bent-to-extended movement occurs by a rotation around a pivot at the Lec-EGF interface and results in a separation of the two domains.

To confirm that ligand binding directly promotes the extended conformation of E-selectin in solution, we employed SAXS as a label-free and sensitive technique for detecting conformational changes. Calculated SAXS curves reveal a small but characteristic difference between models of the apo-E-selectin* bent and the ligand-bound extended conformation at $q = 0.3–0.4$ Å^{-1} (black and red lines in Figure 4A and B). Indeed, the experimental scattering curve for E-selectin* in absence of ligand is in good agreement only with the calculated curve for the apo-E-selectin* model, whereas the scattering curve in the presence of glycomimetic **1** exhibits the expected shift at $q = 0.3–0.4$ Å^{-1} and correlates well with the E-selectin*/**1** model (Figure 4B). These results demonstrate that the solution conformation closely resembles the conformation in the crystal structures. Ligand binding therefore indeed shifts the conformational equilibrium of E-selectin from the bent to the extended state, while the linear arrangement of SCR domains is maintained irrespective of the presence or absence of the ligand.

We employed molecular dynamics simulations to calculate relative binding free energies for the bent and extended conformation of E-selectin and, due to limitations of the method (see Supplementary material for details), scaled the absolute values according to our previously reported data from isothermal titration calorimetry (Binder et al., 2012). The obtained difference of 0.82 kcal/mol for the binding of the natural sLe^x ligand demonstrates that additional interactions of protein and ligand in the extended conformation

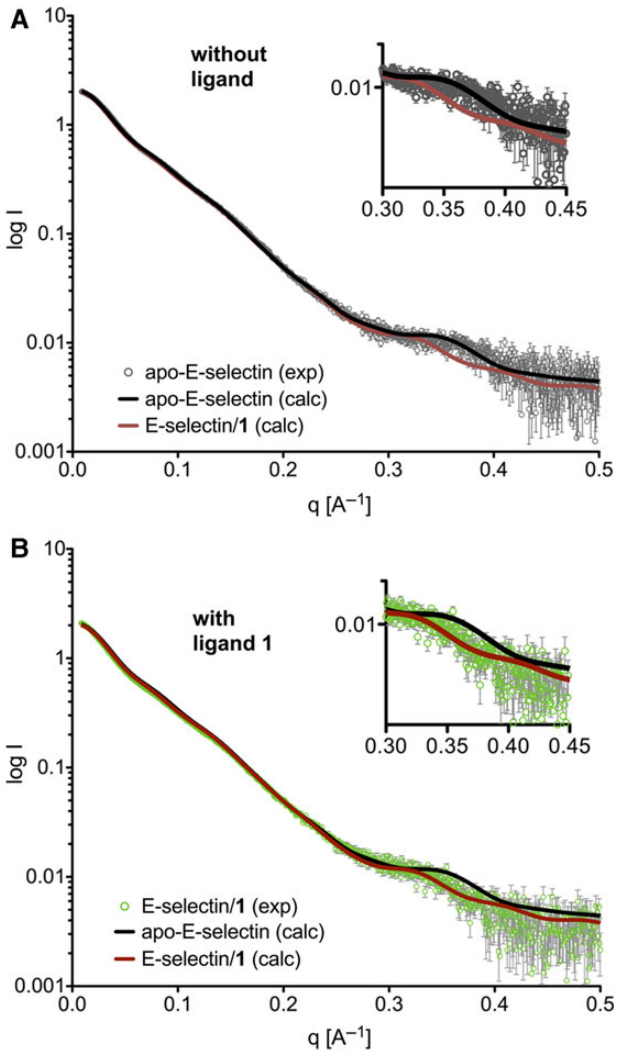

Figure 4 In solution SAXS analysis reveals the conformational differences between apo-E-selectin and the E-selectin/**1** complex. (**A** and **B**) Calculated (black or red lines) and experimental (circles) scattering curves of E-selectin in absence (gray circles) or presence (green circles) of the ligand. Error bars correspond to the standard error of the means of eleven measurement points. (**A**) In absence of glycomimetic **1**, E-selectin adopts the bent conformation. (**B**) In presence of the ligand, the experimental scattering curve shows a significant shift at $q = 0.3–0.4$ Å^{-1} corresponding to a transition toward the extended conformation.

result in higher interaction energies in comparison to the shallow binding site in the bent state (Supplementary Table S4). This change in binding free energy translates into a four-fold increase in the dissociation constant (K_D) and supports the notion that the extended conformation represents a true high-affinity binding state of E-selectin.

The conformational coupling mechanism of E-selectin

Alterations in the Lec domain connect ligand binding to conformational change. Three regions located in the Lec domain are affected by conformational changes upon ligand binding: The

binding site loop 81–89 changes its conformation (Figure 5A), and a bridging region formed by two loops (residues 52–75) transduces this motion (Figure 5B) to the pivot region consisting of the pivot residue Trp1 (Figure 5C) and surrounding residues in the Lec (residues 22–23 and 30–31, Figure 5C and D) and in the EGF-like domain (Asn138). These variable regions are mounted onto a rigid scaffold of the Lec domain, stabilized by two disulfide bonds (Cys19–Cys117 and Cys90–Cys109). The alterations extend over

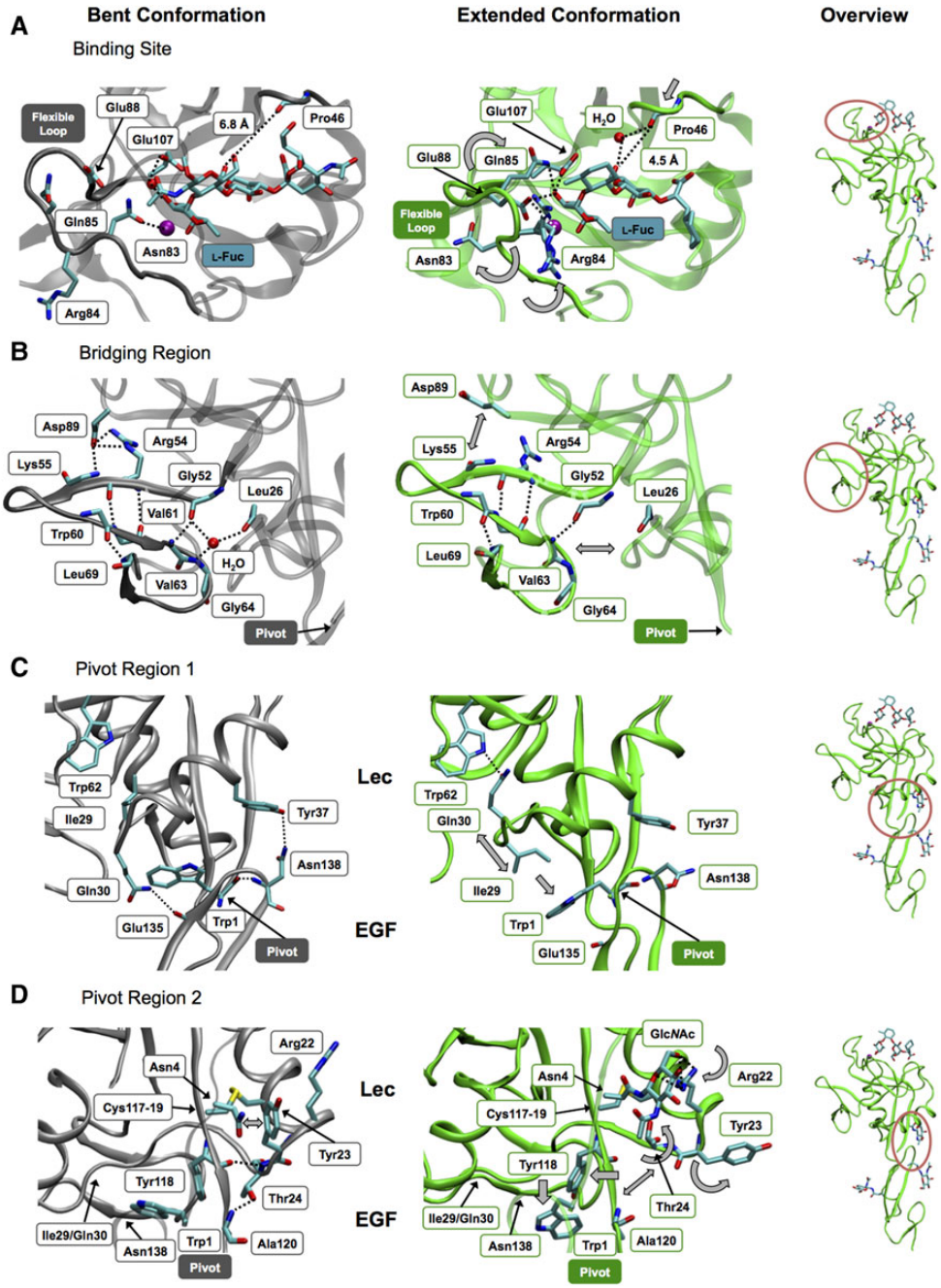

Figure 5 The bent and extended conformation of E-selectin exhibit differences in the ligand-binding site reaching to the Lec-EGF domain interface. (**A**) The binding site is constricted by rearrangements of loop 81–89. Glu88 replaces Asn83 as Ca^{2+} coordinating residue and forms an additional interaction with the 2-hydroxyl group of L-Fuc. (**B**) The bridging region 52–70 undergoes a rigid body motion breaking the interactions of Arg54/Lys55 with Asp89 of the binding site. At the pivot interface, a water-mediated hydrogen bond network involving Gly52, Val63, and Leu26 is perturbed. (**C**) Within the pivot region, Ile29 and Gln30 flip orientation, which disrupts interdomain interactions to Glu135 and favors a dislocation of Trp1, leading to the hinge-bending motion between the Lec and EGF domains. The Tyr37–Asn138 interdomain interaction is broken. (**D**) Another shift in the pivot region originates at the Glc*N*Ac residue linked to Asn4. The interaction of Arg22 with the carbohydrate further disrupts interdomain interactions and releases the Tyr118 side chain toward the pivot residue Trp1.

35 Å from the carbohydrate-binding site to the interface with the EGF-like domain.

The ligand-binding site. The most extensive conformational changes are observed within the binding site loop 81–89 (Figure 5A), where the Cα atom of residue Gln85 moves by 10 Å (see Supplementary Video S2). This leads to a constriction around the central Ca^{2+} ion and the L-fucose (L-Fuc) moiety of the ligand, which coordinates the Ca^{2+} ion with its 3- and 4-hydroxyl groups. In the bent conformation Asn83 coordinates the Ca^{2+} ion, while in the extended conformation Glu88 swings inwards to coordinate the Ca^{2+} ion and displaces Asn83 toward the solvent. This swapping is supported by an additional interaction between Glu88 and the 2-hydroxyl group of L-Fuc. Gln85, which is solvent-exposed in the bent conformation, also shifts toward the ligand into hydrogen bonding distance to the 2-hydroxyl group. Thus, as a consequence of the conformational adaptation, the 2-hydroxyl group of L-Fuc directly interacts with the protein in the extended conformation, while it is only involved in water-mediated interactions to Glu107 and Asn83 in the bent conformation. These findings explain the importance of the L-Fuc 2-hydroxyl group for ligand affinity (Brandley et al., 1993; Ramphal et al., 1994), which was not rationalized by earlier structural data (Somers et al., 2000). Finally, also the loop around Pro46 shifts from an original distance of 6.8 Å to the 6-hydroxyl group of the D-galactose (D-Gal) moiety in the bent conformation toward 4.5 Å in the extended conformation, where the backbone oxygen of Pro46 mediates a water-bridged interaction to the 6-hydroxyl group of D-Gal.

The bridging region. The constriction around the L-Fuc binding site leads to the disruption of interactions at the interface of the binding site and the bridging loops 52–75 (Figure 5B) between the Asp89 and Arg54 side chains and Lys55 backbone, respectively. The bridging region itself shifts in a rigid body motion from the bent to the extended conformation. This rigidity is maintained by backbone interactions between Arg54 and Trp60/Val61, Gly52 and Val63 as well as Trp60 and Leu69. The rigid body motion serves as an allosteric bridge for transmitting the conformational alteration from the binding site to the pivot region.

The pivot region. The E-selectin bent conformation is stabilized by an extensive hydrogen bond network between the Lec and EGF-like domains with main contributions from Trp1, Thr24, Gln30, Tyr37, Ala120, Glu135, and Asn138 (Figure 5C and D). The Trp1 hinge residue is the only residue of the Lec domain that coherently moves with the EGF-like domain to the extended conformation. This motion is accompanied by (i) a flip of residues Ile29/Gln30 (Figure 5C), (ii) a flip of residues Tyr23/Thr24 accompanied by an altered side chain conformation of Arg22 (Figure 5D), and (iii) a disruption of the interdomain interaction between Tyr37/Asn138 (Figure 5C). A flip of the residues Ile29 and Gln30, located in a solvent exposed loop with increased flexibility between helix 1 and 2 of the Lec domain, facilitates the movement of Trp1 (Figure 5C). In the bent conformation, Ile29 is enclosed in a hydrophobic pocket, while Gln30 is involved in intra- and interdomain interactions to Glu34 and Glu135. When the extended conformation is adopted, the steric hindrance of Trp1 on Ile29 and Gln30 is released and the flipped conformation of Gln30 is stabilized by new interactions with the backbone oxygen of Gly102 and the side chain of Trp104. These rearrangements in the pivot region disrupt a contact to the bridging region mediated by a water molecule bridging the backbone of Leu26 to Gly52/Gly64 (Figure 5B). As a consequence, the pivot and bridging regions are further separated and additional water molecules enter into the crevice between the domains. Tyr23 and Thr24 are restrained in the bent conformation by the side chain of Arg22. While Arg22 stacks with Tyr18 in the bent conformation, its side chain is re-oriented in the extended conformation and interacts with the Glc*N*Ac attached to Asn4. The movement of Arg22 provides space for a flip of residues Tyr23 and Thr24 of the pivot region (Figure 5D). Tyr23 relaxes from an unfavorable into a favorable position in the Ramachandran plot. The new conformation is stabilized by an interaction of the Thr24 side chain with the Cys19 backbone oxygen. The flip of Tyr23/Thr24 further disrupts interactions between the Lec and EGF-like domains, namely between Thr24 backbone and Tyr118 backbone and Thr24 side chain with Ala120. The side chain of Tyr118 enters into a cleft that is opened by the movement of Trp1. A hydrogen bond between Tyr37 and Asn138 contributes to the interface between the Lec and EGF-like domains in the bent conformation of E- and L-selectin (PDB code 3CFW). In the E-selectin*/**1** structure, the Asn138 residue is pushed toward the Lec domain, thus disrupting the interdomain hydrogen bond to Tyr37 (Figure 5C). This conformational change is additionally accompanied by a backbone flip between Ile137 and Asn138.

Comparative analysis of mechanocoupling in E- and P-selectin

A transition from bent to extended conformation in selectins has previously been observed only for the Lec-EGF didomain of P-selectin co-crystallized with a multivalent PSGL-1 peptide ligand (Somers et al., 2000). This peptide comprised the 19 N-terminal amino acids of mature PSGL-1, including an sLe^x-modified glycan attached to Thr16 and three sulfated tyrosine residues, which are directly involved in protein ligand interactions (Sako et al., 1995; Wilkins et al., 1995; Somers et al., 2000). Based on the P-selectin/PSGL-1 crystal structure, a P-selectin-specific mechanism for conformational coupling was proposed (Springer, 2009). Despite a sequence identity in the Lec and EGF-like domains of 62% between E- and P-selectin (Supplementary Figure S6), two key differences between E- and P-selectin supported the P-selectin-specificity of the proposed mechanism: First, E-selectin does not interact with sulfated tyrosines, while those mediate key protein–ligand interaction in the P-selectin/PSGL-1 complex (Li et al., 1996; Rodgers et al., 2000). Second, differences in the Lec-EGF domain interface suggested a stabilization of the bent conformation in E-selectin by an additional hydrogen bond (Graves et al., 1994; Somers et al., 2000). The current data demonstrate that E- and P-selectin undergo a similar overall conformational change, but with considerable differences in the mechanism of conformational coupling. (i) The E-selectin Lec-EGF domain interface is locked by a hydrogen

bond between Asn138 and Tyr37. This interaction is absent in P-selectin, which carries a glycine at position 138. The functional relevance of this interdomain interaction was demonstrated on L-selectin, where an Asn138Gly mutant improved ligand binding under hydrodynamic force (Lou et al., 2006; Phan et al., 2006). It has been hypothesized, that Asn138 would be forced into an unfavorable backbone conformation upon disruption of the Tyr37-Asn138 hydrogen bond, which would finally prevent the transition into the extended state (Springer, 2009). The backbone flip between residues 137 and 138 observed here, now demonstrates how such non-favored conformation is avoided. (ii) While the Trp1 residue has also been identified as the pivot for P-selectin, the flip of the Ile29 and Gln30 side chains was not observed. (iii) Residue Tyr23 in the direct vicinity of the pivot residue Trp1 is unaltered in the bent and extended conformation of P-selectin, while it relaxes from an unfavorable into a favorable backbone conformation for E-selectin.

Discussion

The catch-bond behavior of selectins is crucial for their ability to mediate leukocyte rolling and is achieved by a transition between a bent and an extended conformational state (Marshall et al., 2003; Waldron and Springer, 2009; Snook and Guilford, 2010; Wayman et al., 2010). This has been elegantly demonstrated by forcing P-selectin into an extended conformation by modifications at the Lec-EGF interface: A P-selectin variant locked in an extended conformation displays enhanced ligand binding under static conditions, but its ability to mediate leukocyte rolling under flow conditions was impaired (Phan et al., 2006; Waldron and Springer, 2009). However, an extended conformation has so far only been observed for P-selectin in complex with a glycopeptide ligand that interacts with its carbohydrate epitope as well as three sulfated tyrosines. Here, we reveal an extended state of E-selectin in complex with its minimal binding motif sLe^x. Based on an analysis of protein–ligand interactions and quantitative analysis of molecular dynamics simulations, this extended conformation represents a true high-affinity ligand-binding state of E-selectin. With SAXS measurements we demonstrate for the first time for any selectin, that small-molecule ligand-binding induces a conformational transition from the bent low affinity to the extended high-affinity state in solution. Therefore, glycoprotein ligands such as PSGL-1 or ESL-1 are not strictly required for efficiently promoting conformational changes in selectins. Even a small molecular ligand such as sLe^x in the absence of flow conditions is sufficient to initiate a structural transition to an extended conformation.

To analyze the functional mechanisms underlying catch-bond behavior, detailed structural knowledge of all relevant states of E-selectin is required (Figure 6). Apo-E-selectin adopts a bent conformation of the Lec-EGF didomain as demonstrated by crystallographic analysis (Graves et al., 1994) and SAXS data. The bent conformation is capable of recognizing and weakly binding sLe^x, as demonstrated in a crystallographic ligand soaking experiment, where crystal packing restraints prevented the transition to the extended conformation (Somers et al., 2000). However, in solution ligand binding results in a conformational transition into the extended high-affinity binding state revealed here by co-crystallization and SAXS. The conformational change from a bent to an extended conformation allows E-selectin to support fast binding of rapidly flowing leukocytes to the vascular endothelium at the leading edge of the cell while controlling the rate of unbinding at the trailing edge, thus providing mechanical stability to the rolling of leukocytes along the vasculature. Under *in vivo* flow conditions, the extended conformation is favored by tensile force pulling along the E-selectin–ligand axis reinforcing the extended conformation and thus increasing lifetime of the interaction. The rigidity of the linearly arranged SCR domains is promoted by conserved interdomain contacts and three intradomain disulfide bonds and provides a basis for mechanosensing by the Lec-EGF didomain of E-selectin. Our findings provide direct evidence for the two-state-two-pathway model of conformational changes underlying catch-bond properties in E-selectin (Figure 6). The bent conformation is prevailing in solution and recognizes ligands in a low-affinity encounter complex. The encounter complex undergoes a conformational change to a high-affinity extended state already under no-force conditions, but tensile force acting along the Lec-EGF–ligand-binding site axis further increases its lifetime. Such a two-state-two-pathway model has been previously proposed for the P-selectin/PSGL-1 complex (Evans et al., 2004), for the bacterial adhesin FimH in complex with mannose (Thomas et al., 2006), and most recently for the cadherin-catenin complex binding to actin filaments (Buckley et al., 2014). So far, P-selectin was the only system for which two distinct ligand-bound states have been structurally characterized, but with very different low- (sLe^x) and high-molecular weight (PSGL-1) ligands (Somers et al., 2000). Our current data together with the previous low-affinity E-selectin/sLe^x structure (Somers et al., 2000) provide for the first time a comprehensive view on the full set of apo- as well as low- and high-affinity structures underlying the catch-bond behavior with one and the same natural ligand.

The ligand-binding site of E-selectin undergoes dramatic conformational changes between the low-affinity and the high-affinity state (Supplementary Video S1). The shallow binding surface is transformed into a pronounced binding pocket with multiple additional protein–ligand interactions, while the conformation of the ligand remains unchanged. Co-crystallization with the glycomimetic **1** demonstrates the relevance of the high-affinity conformation for the design of drug candidates targeting E-selectin. The detailed knowledge into ligand recognition of E- and P-selectin opens the way toward the rational design of novel E-selectin-specific antagonists. Based on the success of the pan-selectin antagonist Rivipansel, E-selectin-specific antagonists are promising drug candidates that may further target specific indications related to excessive inflammatory responses in human disease. In summary, the current results contribute to a comprehensive understanding of the mechanism of mechanosensing and catch-bond behavior in the selectin family and they reveal the pathway of ligand-induced conformational changes in E-selectin with critical relevance for ongoing targeted drug discovery.

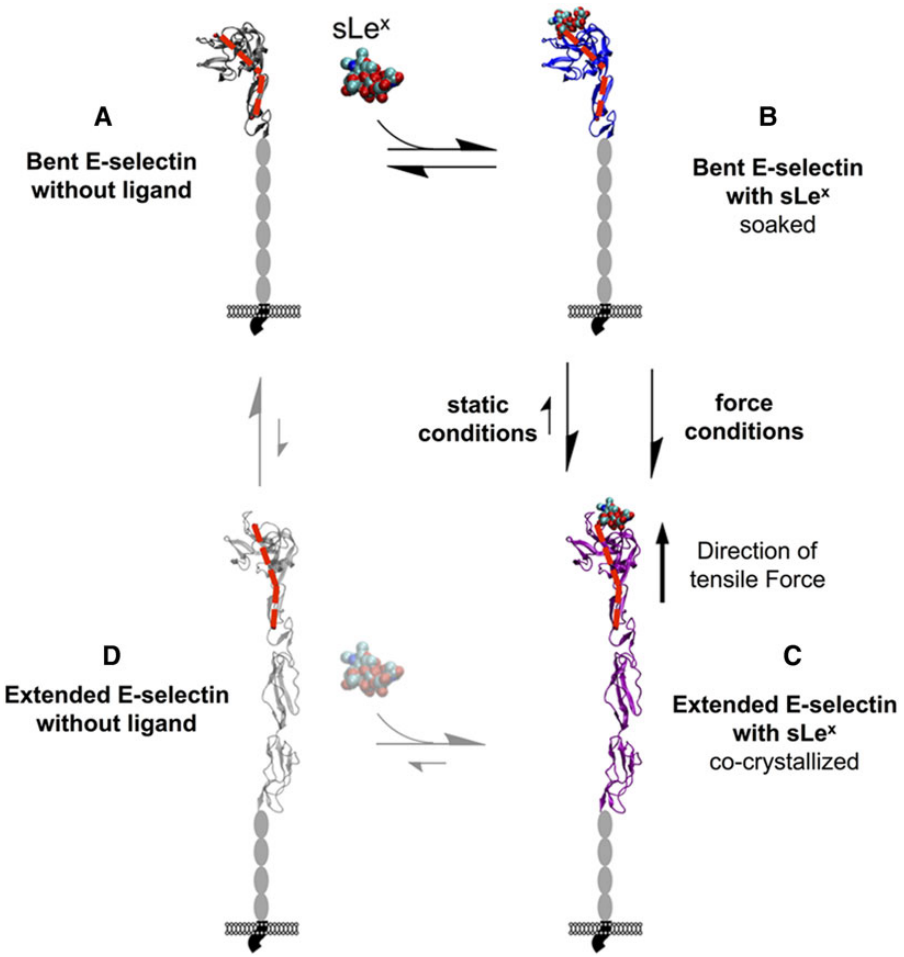

Figure 6 The ligand-dependent equilibrium between bent and extended conformation of E-selectin. In absence of ligand, E-selectin primarily adopts the bent conformation (**A**) and not an extended conformation (**D**). The bent conformation is capable of ligand binding (**B**), although with low affinity. Upon ligand binding E-selectin favors the extended high-affinity state (**C**). Tensile force along the E-selectin–ligand axis exerted by tethered leukocytes under flow conditions increases the lifetime of the high-affinity conformation.

Materials and methods

Ligand synthesis

The glycomimetic **1** {(1*R*,2*R*,3*S*)-2-[(α-L-fucopyranosyl)oxy]-3-methyl-cyclohex-1-yl} 3-O-[sodium (1*S*)-1-carboxy-2-cyclohexyl-ethyl]-β-D-galactopyranoside was synthesized as reported previously (Schwizer et al., 2012). The tetrasaccharide trimethylsilylethyl sialyl Lewis^x (sLe^x-OTMSE) was synthesized as described in Supplementary material.

Protein expression and purification

The coding sequences of the human E-selectin Lec-EGF-SCR1+2 domains (E-selectin*) cDNA were cloned into the pcDNA3.1(+) expression vector (Life Technologies Ltd) using standard procedures. Stably transfected CHO-K1 cells (ATCC-No. CCL-61) were generated using FuGENE® HD (Roche Applied Science) transfection, G418 treatment, and subsequent clone selection. Protein expression was carried out in monolayer cultures in the presence of kifunensine. Purification using the functional anti-E-selectin antibody 7A9 coupled to sepharose was carried out as described previously (Binder et al., 2012). Concentrated high-mannosylated E-selectin was partially deglycosylated with endoglycosidase H yielding protein with seven single Glc*N*Ac moieties attached to each *N*-linked glycosylation site. For details see Supplementary material.

Co-crystallization and structure determination

Deglycosylated E-selectin* was co-crystallized with sLe^x-OTMSE or glycomimetic **1** in a sitting drop setup in the presence of 0.2 M $CaCl_2$ using polyethylene glycol 8000 as precipitant. Plate-like crystals appeared within 1 day after seeding. The structures of E-selectin*/**1** and E-selectin*/sLe^x were determined by molecular replacement and refined using BUSTER (Blanc et al., 2004). For details on data collection and refinement see Supplementary material (Supplementary Table S1).

Small-angle X-ray scattering

SAXS measurements were conducted at beamline x12sa-cSAXS of the Swiss Light Source using partially deglycosylated E-selectin* in presence or absence of 3 mM glycomimetic **1**. Experimental data were processed with PRIMUS (Konarev et al., 2003) and theoretical

scattering curves were evaluated with CRYSOL (Svergun et al., 1995). A model for the E-selectin* bent conformation was generated using the coordinates of the apo-form of the E-selectin Lec-EGF didomain (Graves et al., 1994) combined with the coordinates of the two SCR domains from E-selectin*/**1**. For details see Supplementary material (Supplementary Table S2).

Molecular dynamics simulations

Molecular dynamics simulations were carried out using the OPLS 2005 force field at a constant temperature of 300 K. Energetic and structural data were recorded in 4.8 ps intervals. From the collected frames, every tenth (1000 frames in total) was used to calculate the average ΔG applying the molecular mechanics generalized Born surface area (MM-GBSA) method. The details are described in Supplementary material (Supplementary Tables S3 and S4).

Supplementary material

Supplementary material is available at *Journal of Molecular Cell Biology* online.

Acknowledgements

The authors thank the staff of beamline PXIII, Andreas Menzel from the Swiss Light Source, Paul Scherrer Institute, Villigen, Switzerland, and Rudi Glockshuber and Maximilian Sauer (ETH Zürich) for support of fluorescence measurements.

Funding

This work was supported by the Swiss National Science Foundation (grant number 200020_129935 and R'EQUIP 145023).

Conflict of interest: none declared.

References

Beste, M.T., and Hammer, D.A. (2008). Selectin catch-slip kinetics encode shear threshold adhesive behavior of rolling leukocytes. Proc. Natl Acad. Sci. USA *105*, 20716–20721.

Binder, F.P., Lemme, K., Preston, R.C., et al. (2012). Sialyl Lewis(x) : a 'pre-organized water oligomer'? Angew. Chem. Int. Ed. Engl. *51*, 7327–7331.

Blanc, E., Roversi, P., Vonrhein, C., et al. (2004). Refinement of severely incomplete structures with maximum likelihood in BUSTER-TNT. Acta Crystallogr. D Biol. Crystallogr. *60*, 2210–2221.

Brandley, B.K., Kiso, M., Abbas, S., et al. (1993). Structure-function studies on selectin carbohydrate ligands—modifications to fucose, sialic-acid and sulfate as a sialic-acid replacement. Glycobiology *3*, 633–641.

Buckley, C.D., Tan, J.Y., Anderson, K.L., et al. (2014). The minimal cadherin-catenin complex binds to actin filaments under force. Science *346*, 1254211.

Clinicaltrials.gov. (2014a). Study of GMI-1070 for the treatment of sickle cell pain crisis. https://clinicaltrials.gov/ct2/show/NCT01119833?term=rivipansel: Clinicaltrials.gov, Identifier NCT01119833.

Clinicaltrials.gov. (2014b). Study of intravenous GMI-1070 in adults with sickle cell disease. https://clinicaltrials.gov/ct2/show/NCT00911495?term=rivipansel: Clinicaltrials.gov, Identifier NCT00911495.

Crothers, J.M., Jr, Asano, S., Kimura, T., et al. (2004). Contribution of oligosaccharides to protection of the H,K-ATPase beta-subunit against trypsinolysis. Electrophoresis *25*, 2586–2592.

Erbe, D.V., Wolitzky, B.A., Presta, L.G., et al. (1992). Identification of an E-selectin region critical for carbohydrate recognition and cell-adhesion. J. Cell Biol. *119*, 215–227.

Evans, E., Leung, A., Heinrich, V., et al. (2004). Mechanical switching and coupling between two dissociation pathways in a P-selectin adhesion bond. Proc. Natl Acad. Sci. USA *101*, 11281–11286.

Finger, E.B., Puri, K.D., Alon, R., et al. (1996). Adhesion through L-selectin requires a threshold hydrodynamic shear. Nature *379*, 266–269.

Graves, B.J., Crowther, R.L., Chandran, C., et al. (1994). Insight into E-selectin/ligand interaction from the crystal structure and mutagenesis of the lec/EGF domains. Nature *367*, 532–538.

Imperiali, B., and O'Connor, S.E. (1999). Effect of N-linked glycosylation on glycopeptide and glycoprotein structure. Curr. Opin. Chem. Biol. *3*, 643–649.

Kansas, G.S. (1996). Selectins and their ligands: current concepts and controversies. Blood *88*, 3259–3287.

Konarev, P.V., Volkov, V.V., Sokolova, A.V., et al. (2003). PRIMUS: a Windows PC-based system for small-angle scattering data analysis. J. Appl. Crystallogr. *36*, 1277–1282.

Kundra, R., and Kornfeld, S. (1999). Asparagine-linked oligosaccharides protect Lamp-1 and Lamp-2 from intracellular proteolysis. J. Biol. Chem. *274*, 31039–31046.

Lasky, L.A. (1995). Selectin-carbohydrate interactions and the initiation of the inflammatory response. Annu. Rev. Biochem. *64*, 113–139.

Ley, K. (2003). The role of selectins in inflammation and disease. Trends Mol. Med. *9*, 263–268.

Li, S.H., Burns, D.K., Rumberger, J.M., et al. (1994). Consensus repeat domains of E-selectin enhance ligand binding. J. Biol. Chem. *269*, 4431–4437.

Li, F.G., Wilkins, P.P., Crawley, S., et al. (1996). Post-translational modifications of recombinant P-selectin glycoprotein ligand-1 required for binding to P- and E-selectin. J. Biol. Chem. *271*, 3255–3264.

Lou, J.Z., and Zhu, C. (2007). A structure-based sliding-rebinding mechanism for catch bonds. Biophys. J. *92*, 1471–1485.

Lou, J.Z., Yago, T., Klopocki, A.G., et al. (2006). Flow-enhanced adhesion regulated by a selectin interdomain hinge. J. Cell Biol. *174*, 1107–1117.

Marshall, B.T., Long, M., Piper, J.W., et al. (2003). Direct observation of catch bonds involving cell-adhesion molecules. Nature *423*, 190–193.

Pereverzev, Y.V., Prezhdo, O.V., Forero, M., et al. (2005). The two-pathway model for the catch-slip transition in biological adhesion. Biophys. J. *89*, 1446–1454.

Phan, U.T., Waldron, T.T., and Springer, T.A. (2006). Remodeling of the lectin–EGF-like domain interface in P- and L-selectin increases adhesiveness and shear resistance under hydrodynamic force. Nat. Immunol. *7*, 883–889.

Phillips, M.L., Nudelman, E., Gaeta, F.C., et al. (1990). ELAM-1 mediates cell adhesion by recognition of a carbohydrate ligand, sialyl-Lex. Science *250*, 1130–1132.

Polley, M.J., Phillips, M.L., Wayner, E., et al. (1991). CD62 and endothelial cell-leukocyte adhesion molecule 1 (ELAM-1) recognize the same carbohydrate ligand, sialyl-Lewis x. Proc. Natl Acad. Sci. USA *88*, 6224–6228.

Prota, A.E., Sage, D.R., Stehle, T., et al. (2002). The crystal structure of human CD21: implications for Epstein-Barr virus and C3d binding. Proc. Natl Acad. Sci. USA *99*, 10641–10646.

Ramachandran, V., Nollert, M.U., Qiu, H.Y., et al. (1999). Tyrosine replacement in P-selectin glycoprotein ligand-1 affects distinct kinetic and mechanical properties of bonds with P- and L-selectin. Proc. Natl Acad. Sci. USA *96*, 13771–13776.

Ramphal, J.Y., Zheng, Z.L., Perez, C., et al. (1994). Structure-activity-relationships of sialyl-Lewis x-containing oligosaccharides .1. Effect of modifications of the fucose moiety. J. Med. Chem. *37*, 3459–3463.

Rodgers, S.D., Camphausen, R.T., and Hammer, D.A. (2000). Sialyl Lewis(x)-Mediated, PSGL-1-independent rolling adhesion on P-selectin. Biophys. J. *79*, 694–706.

Rodriguez-Romero, A., Almog, O., Tordova, M., et al. (1998). Primary and tertiary structures of the Fab fragment of a monoclonal anti-E-selectin 7A9 antibody that inhibits neutrophil attachment to endothelial cells. J. Biol. Chem. *273*, 11770–11775.

Sako, D., Comess, K.M., Barone, K.M., et al. (1995). A sulfated peptide segment at the amino-terminus of PSGL-1 is critical for P-selectin binding. Cell *83*, 323–331.

Sarangapani, K.K., Yago, T., Klopocki, A.G., et al. (2004). Low force decelerates L-selectin dissociation from P-selectin glycoprotein ligand-1 and endoglycan. J. Biol. Chem. *279*, 2291–2298.

Schwizer, D., Patton, J.T., Cutting, B., et al. (2012). Pre-organization of the core structure of E-selectin antagonists. Chemistry *18*, 1342–1351.

Snook, J.H., and Guilford, W.H. (2010). The effects of load on E-selectin bond rupture and bond formation. Cell. Mol. Bioeng. *3*, 128–138.

Somers, W.S., Tang, J., Shaw, G.D., et al. (2000). Insights into the molecular basis of leukocyte tethering and rolling revealed by structures of P- and E-selectin bound to SLe(X) and PSGL-1. Cell *103*, 467–479.

Springer, T.A. (2009). Structural basis for selectin mechanochemistry. Proc. Natl Acad. Sci. USA *106*, 91–96.

Svergun, D., Barberato, C., and Koch, M.H.J. (1995). CRYSOL—a program to evaluate x-ray solution scattering of biological macromolecules from atomic coordinates. J. Appl. Crystallogr. *28*, 768–773.

Thomas, W., Forero, M., Yakovenko, O., et al. (2006). Catch-bond model derived from allostery explains force-activated bacterial adhesion. Biophys. J. *90*, 753–764.

Thomas, W.E., Vogel, V., and Sokurenko, E. (2008). Biophysics of catch bonds. Annu. Rev. Biophys. *37*, 399–416.

Waldron, T.T., and Springer, T.A. (2009). Transmission of allostery through the lectin domain in selectin-mediated cell adhesion. Proc. Natl Acad. Sci. USA *106*, 85–90.

Walz, G., Aruffo, A., Kolanus, W., et al. (1990). Recognition by ELAM-1 of the sialyl-Lex determinant on myeloid and tumor cells. Science *250*, 1132–1135.

Wayman, A.M., Chen, W., McEver, R.P., et al. (2010). Triphasic force dependence of E-selectin/ligand dissociation governs cell rolling under flow. Biophys. J. *99*, 1166–1174.

Wilkins, P.P., Moore, K.L., Mcever, R.P., et al. (1995). Tyrosine sulfation of P-selectin glycoprotein ligand-1 is required for high-affinity binding to P-selectin. J. Biol. Chem. *270*, 22677–22680.

Yakovenko, O., Sharma, S., Forero, M., et al. (2008). FimH forms catch bonds that are enhanced by mechanical force due to allosteric regulation. J. Biol. Chem. *283*, 11596–11605.

Zhu, C., Yago, T., Lou, J., et al. (2008). Mechanisms for flow-enhanced cell adhesion. Ann. Biomed. Eng. *36*, 604–621.